Al Azhar Buletin of Science Vol.(26) No.1, June, 69 - 84, 2015.

MINERALOGY AND RADIOACTIVITY STUDIES OF WADI YOIDER STREAM SEDIMENTS, SOUTH EASTERN DESERT, EGYPT

MOUSTAFA, B. BAYOUMI, EL AZAB, A., AND KHALED EL HOSSINY

ABSTRACT

Wadi Yoider area is located in the South Eastern Desert of Egypt, covering an area of about 150km2. It is covered by basement rocks dissected by Wadi Yoider as a main wadi with several tributaries. The rock types cropping out at Wadi Yoider area comprise, from the oldest to youngest, metavolcanics, younger gabbros, alkali feldspar granites, muscovite granites, biotite granites, monzogranites, and wadi deposits (quaternary sediments) filling the streams of the studied area. The results of the sedimentological statistical parameters are graphic mean (Mz) indicate that, they range from 0.04 to 1.8 with average 0.85, inclusive graphic standard deviation (σI) ranging from 0.88 to 1.8 with an average 1.2, inclusive graphic skewness (SkI) ranging from 0.03 to 0.33 with an average 0.2, and inclusive graphic kurtosis (Kg) ranging from 0.68 to 2.05 with an average 1.4. These samples are characterized by fine skewed, neer skewed, coarse skewed, platykurtic and mesokurtic. All these features indicate of a turrstile. Gravity and magnetic separation techniques in addition to microscopic examination for the studied stream sediment samples were applied to identify the heavy minerals in these sediments. These minerals are represented by magnetite, ilmenite, hematite, rutile, leucoxene, garnet, titanite, zircon, and samarskite. The average concentrations of U and Th in the stream sediments of Wadi Yoider are 20.2ppm and 42.2ppm, which are higher than the clarke values for earth crust.

INTRODUCTION

Wadi Yoider area is located in the Southern Eastern Desert of Egypt between longitudes 36° 08`E and 36° 17`E and Latitudes 22° 13`N and 22° 20`N (Figure 1). The area under investigation studied by different authors eg. Stern et al., (1984) and El-Gaby et al., (1988). El Sela pluton are the most promising uranium occurrence in the Southern Eastern Desert of Egypt because of the abnormal high contents of uranium. The studied area covering about 150km^2 (Figure 1). This area is characterized by rugged topography with moderate to high relief and very arid climate. The present work is concerned with heavy minerals concentrations of Wadi Yoider stream sediments as well as their content of uranium and thorium. The basement rocks in Wadi Yoider area are of Precambrian age and dissected by dry wadis that filled by a wide variety of stream sediments (wadi deposits).

The studies stream sediments accumulations in the form of alluvial fans. Wadi deposits are composed of sands, gravels, boulders contain some heavy valuable minerals, derived from alkali feldspar granites, muscovite granites, biotite granites, and monzogranites.

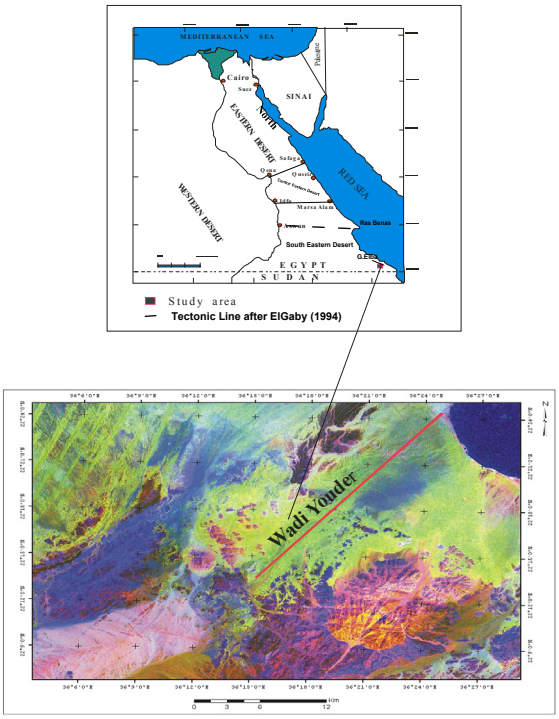

Figure 1 Location Map of the study area

Geological setting

Stern et al., (1984) and El-Gaby et al., (1988) recognized three domains in the Eastern Desert of Egypt which show a significant variations in the nature of the exposed igneous rock suites and their tectonic styles. The first domain, extends from the Egyptian-Sudanese border northward

to approximately the Ras Benas-Aswan line. It is characterized by the presence of ophiolitic belts and associated linear ultramafics probably marking the location of suture zones, Gabal Elba area is a part of the Arabo-Nubian shield which is composed of the Late Precambrian basement rocks. These rocks have been developed during the Pan African tectono-thermal events (950-550 Ma. Kröner, 1984). **Gaafar** et.al., 2014 considered that El Sela granitic pluton is composed of monzogranites, biotite granites two-mica and muscovite granite trending is the ENE-WSW direction (Figure 2). It is jointed in different directions, and defines low to moderate reliefs. This granite is injected by microgranite, dolerite and bostonite dikes, as well as quartz and jasperoid veins. They are mostly injected along ENE-WSW and/or NNW-SSE to N-S directions which represent the most important tectonic trends for U anomalies in the study area. Pegmatite pockets are found as irregular bodies in two-mica granite. They show slightly higher total radioactivity than two-mica granite.

The field observation proved that the studied granites are highly weathered (Figure 3a), cavernous (Figure 3b) and exposed as moderate to high separately hills which form a circular shape of granite pluton (Figure 3c). The older granite

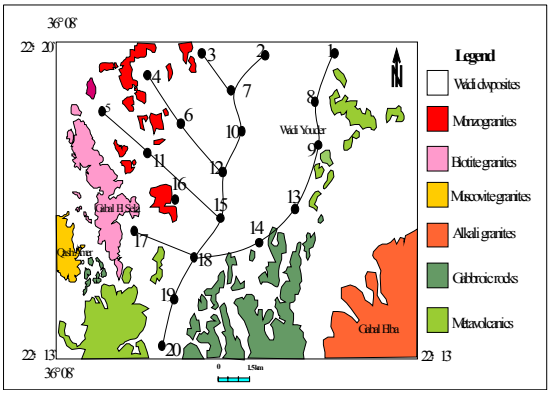

Figure 2 Geological and distribution of samples map of the area

is coarse-grained with a thin peripheral strip of fine grained-granite (monzogranite) with limited exposure (Figure 3d). The second is fine-grained granite, which occurs as smaller intrusion cross-cutting the coarser one (Abdel Meguid et al., 2003). It is reddish pink with manganese oxides filling joints and a fracture as well as disseminations within the rock indicating its suffered from hydrothermal alteration. It is also enriched in pyrite and magnetite. Intensive alteration of the micro-granite to illite and the formation of secondary fluorite and amazonite (green microcline) as well as the complete dissolution of its sulphides.

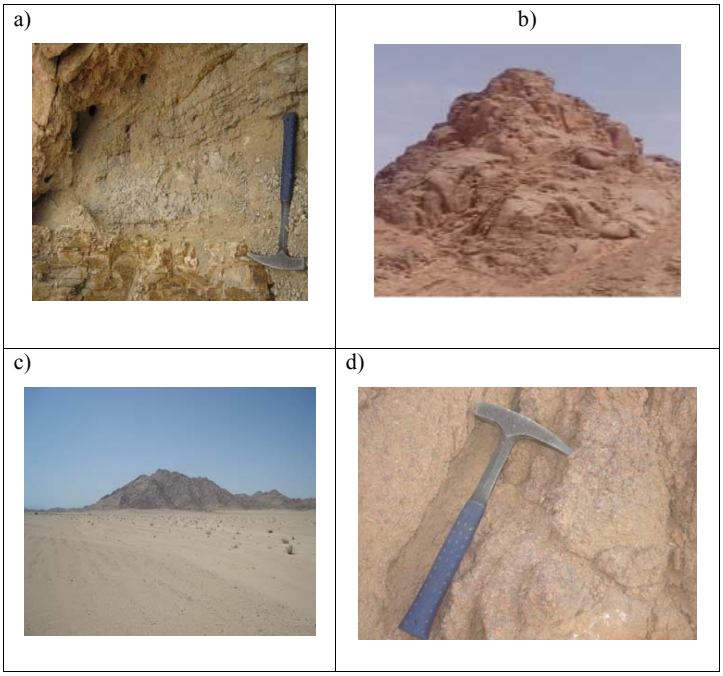

Figure 3 Showing a) highly weathered in granite b) cavernous weathering in granite c) Moderat to high topography of granitic pluton (d Coarse-grained granite

The area is traversed by many wadis, the most important of them is Wadi Yoider. These wadis represent the receivers of the rain water, flushing temporal floods, and the most favorable places to seek the fresh water along these wadis.

The Red Sea coastal plan trends from northwest to southeast. It is quite straight indicating that it belongs to a fault movement mostly related to the Red Sea rift. Along the coast, parallel lines of coral reefs between 50 to 100 meters wide are found. It lies between the Red Sea mountains and the coast. The width of the coastal plain in the studied area varies between 3 km and 8 km.

Materials and Methodology of Study

Samples of the present study were collected from the area around the main Wadi Yoider. Twenty channel samples were collected (Figure 2) from pore holes having about 50cm diameter, and about 0.60-0.8m depth, with intervals ranging from 300-350m. The average weight of each sample is about 7kg.

In order to prepare the samples for study, the air-dried original sample was sieved using a 2 mm screen. The obtained fine fraction was quartered using June's splitters of different chutes, down to about 250 gm. The obtained representative sample was then washed carefully several times accompanied by decantation of the silt and clay fractions. Hydrogen peroxide was used to remove the organic matter.

A representative sub-sample weighting about 60 gm was taken from each prepared sample after quartering and subjected to grain size analysis. The size analysis was carried out using a set of five standard screens selected according to the Wentworth Grade Scale having aperture diameters of 1.0, 0.5, 0.25, 0.125, 0.063 mm.

Separation was conducted using bromoform (Sp. Gr. 2.86g/cm^3) and magnetic fractionation using a Frantz Isodynamic Magnetic Separator (Model L-1). The obtained fractions were carefully studied using the Binocular Stereomicroscope.

In the present study, the collected 20 stream sedimentary samples were analyzed for some trace elements: Rb, Sr, Ba, Ga, Y, Zr, Cu, Zn, Pb, Ni, Co, Cr, V and Nb by XRF techniques on pressed powder pellets.

The spectrometric measurements of eU, eTh, K% and Ra. are performed in part per-million (ppm) units.

The samples are analyzed in cylindrical plastic containers, of volume 212.6 cm^3, 9.5 cm average diameter, and 3 cm length. Then the container was filled with 300–400 gm of the samples, tightly sealed, and left for 30 to accumulate free radon and attain radioactive equilibrium. The four standards U, Th, Ra, and K were measured twice, 1000 seconds for each; the average of gross counts was taken, then divided by their net weight, and introduced to a computer program (Matolin,1990), which runs under Ms-Dos to be used as a matrix of sensitivities represented as the concentrations of U, Th, Ra and K. These concentrations are used as a reference for the studied samples. The latter were measured in the same way by means of the computer program which gives out the concentrations of U and Th in ppm.

RESULTS AND DISCUSSION

Grain Size Analyses

The grain size analysis and its distribution is a fundamental descriptive measure for clastic sediments. It is an important parameter in understanding and interpreting the operative mechanism during transportation and for reflecting the sedimentary environments and the processes of sedimentation, as well as, the dynamics affecting of the area.

The four different sedimentological statistical parameters namely:- the Graphic Mean (M_z), the Inclusive Graphic Standard Deviation (σ_I), the Inclusive Graphic Skewness (Sk_I), and the Graphic Kurtosis (K_G) were calculated for each sample, according to the equations quoted by Folk and Ward (1957) as follow:

-Graphic Mean (M_z) = (ϕ16 + ϕ50 + ϕ84) / 3

-Inclusive Graphic Standard Deviation (σ_I) = [(ϕ84 - ϕ16) / 4] +[ϕ95- ϕ5)/ 6.6]

-Inclusive Graphic Skewness (Sk_I) = [ϕ16 + ϕ84 – 2 ϕ50) / 2(ϕ84 - ϕ16)]

+ [(ϕ5 + ϕ95 - 2ϕ50) / 2(ϕ95 - ϕ5)]

-Graphic Kurtosis (K_G) = (ϕ95 - ϕ5) / 2.44 (ϕ75 - ϕ25)

The obtained results of the grain size distribution of the samples in the studied area clear that the sand size constitutes the main component of all samples, while the clay size, silt size content remove during decantation method.

The grain size parameters (Mz, σ_I, Sk_I, K_G) were calculated, and the results of these parameters are discussed, and described according to the limits of Folk and Ward (1957), and tabulated in (Table 1) as the follow:

The samples have a graphic mean (M_z) ranging from 0.04ϕ to1.8ϕ (Table 1) which means that it lies in coarse and medium sand size classes represented by 70% and 30% respectively (Table 2). The distribution of mean grain size of samples along the study area were represented in histogram (Figure 4a).

The samples have inclusive graphic standard deviation (σ_I) ranging from 0.88 to 1.8 (Table 1), the samples could be categorized in the poorly sorted class and moderately sorted represented by 75% and 25% respectively (Table 2). The distribution of inclusive graphic standard deviation (σ_I) of samples along the study area were represented in histogram (Fig.4b).

The samples have inclusive graphic Skewness (Sk_I) ranging from 0.03 to 0.33 (Table 1), the samples could be categorized in fine skewed, near symmetrical, and strongly fine skewed classes represented by 55% ,40%, and 5% respectively (Table 2). The distribution of inclusive graphic of Skewness (Sk_I) samples along the study area were represented in histogram (Fig. 4c).

The samples have inclusive graphic Kurtosis (K_g) ranging from 0.68 to 2.05 (Table 1), the samples could be categorized in the platykurtic, mesokurtic, very lepto kurtic and lepto kurtic classes represented by 35% , 25% , 15% and 25% respectively (Table 2). The distribution of inclusive graphic kurtosis of samples along the study area were represented in histogram (Figure 4d).

Shape and size are quite important for measuring of the textural maturity of the sediment and the texture as a key of the sedimentary deposit history. So the sorting is reflected the sedimentary history of the deposit. It shows the nature and magnitude of the weathering (transportation, and deposition processes and their duration).The sediments are characterized by poorly to moderately sorted sediment texture and medium to coarse grain size that reflect their immature texture.

The skewness is a measure of the symmetry of the frequency curve. The frequency curve is represented by bolymodal. The bimodal curve may be due to the following:-

a)Effect of source rock: by mechanical weathering of rocks such as granite where two major size are present (medium and coarse), the resulting sediments will have two large amounts related to the two different major sizes (bimodal).

b)Turbulant transportation: Turbidity currents can cause the admixing of sediments from different environments. Turbulent flow is a motion in which velocity fluctuates and direction changes during flow. The material carried is usually of mixed nature and accordingly of less sorted type. The turbulent flow is the ability to carry coarse-grained materials.

Evaluation of Stream Sediments

Heavy minerals distribution

To evaluate the heavy minerals from the studied stream sediment; samples, we should firstly must remove the gangue minerals, especially quartz and feldspars which constitute more than 65% of the stream sediments of Wadi Yoider. The average content of the heavy minerals in the studied stream sediments is 30.86% ranging from 12.8% to 48.5% (Table 3). The content of the heavy minerals in the studied stream sediments increases from south (upstream) to north (downstream).

The common economic heavy minerals in the studied stream sediments are autunite, samarskite, zircon, titanite, monazite, garnet, ru-

Table 1 Grain size parameters of the studied samples

Serial No.	Mean Size (Mz)		Standard Deviation (σ)		Skewness (SKI).		Kurtosis (KG)	
1	1.8	Medium sand	1.7	Poorly sorted	0.16	Fine skewed	0.68	Platy kurtic
2	1.4	Medium sand	1.6	Poorly sorted	0.04	Near symmetrical	0.84	Platy kurtic
3	1.3	Medium sand	1.5	Poorly sorted	0.06	Near symmetrical	0.77	Platy kurtic
4	0.95	Coarse sand	1.4	Poorly sorted	0.17	Fine skewed	0.88	Platy kurtic
5	1.6	Medium sand	1.8	Poorly sorted	0.03	Near symmetrical	0.94	Meso kurtic
6	1.1	Medium sand	1.4	Poorly sorted	0.13	Fine skewed	0.86	Platy kurtic
7	0.8	Coarse sand	1.2	Poorly sorted	0.08	Near symmetrical	1.02	Meso kurtic
8	0.3	Coarse sand	1.1	Poorly sorted	0.05	Near symmetrical	0.82	Platy kurtic
9	0.6	Coarse sand	1.2	Poorly sorted	0.03	Near symmetrical	1.26	Lepto kurtic
10	0.3	Coarse sand	0.92	Moderately sorted	0.23	Fine skewed	1.54	Very lepto kurtic
11	0.04	Coarse sand	1.1	Poorly sorted	0.15	Fine skewed	1.09	Meso kurtic
12	0.05	Coarse sand	1.1	Poorly sorted	0.26	Fine skewed	1.15	Lepto kurtic
13	0.10	Coarse sand	1.8	Poorly sorted	0.21	Fine skewed	1.13	Lepto kurtic
14	0.18	Coarse sand	1.4	Poorly sorted	0.22	Fine skewed	1.11	Meso kurtic
15	0.19	Coarse sand	0.94	Moderately sorted	0.13	Fine skewed	1.59	Very lepto kurtic
16	1.33	Medium sand	1.3	Poorly sorted	0.08	Near symmetrical	0.89	Platy kurtic
17	0.10	Coarse sand	1.3	Poorly sorted	0.33	Strongly fine skewed	1.15	Lepto kurtic
18	0.17	Coarse sand	0.9	Moderately sorted	0.21	Fine skewed	2.05	Very lepto kurtic
19	0.15	Coarse sand	0.97	Moderately sorted	0.15	Fine skewed	1.23	Lepto kurtic
20	0.13	Coarse sand	0.88	Moderately sorted	0.09	Near symmetrical	1.04	Meso kurtic

Table 2 Distribution of the different calculated grain size parameters of the studied samples among the different classes.

Graphic Mean M_z		Inclusive Graphic Standard Deviation (σ_I)		The Inclusive Graphic Skewness (Sk_I)		The Inclusive Kurtosis (K_G):	
Class	%	Class	%	Class	%	Class	%
Coarse sand	70	Poorly sorted	75	Fine skewed	55	Platykurtic	35
Medium sand	30	Moderately sorted	25	Near symmetrical	40	Mesokurtic	25
				Strongly fine skewed	5	Very lepto kurtic	15
						Lepto kurtic	25

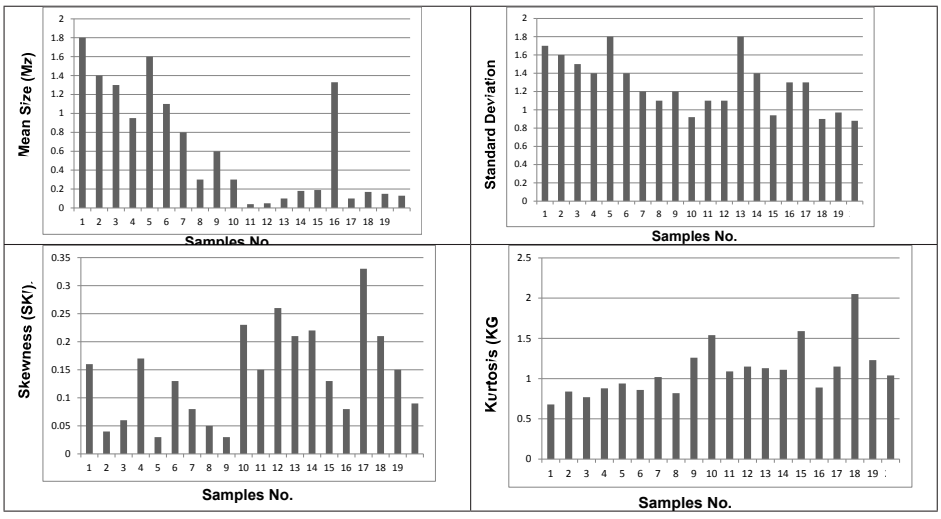

Figure 4 Histograms showing the distribution of a) Graphic mean M_z b) Inclusive graphic standard deviation (σ_I) c) Inclusive graphic skewness (Sk_I) d) Inclusive kurtosis (K_G)

tile, magnetite, and ilmenite in addition to green silicates (Table 4).

Magnetite (Fe_2O_3)

Magnetite was picked by hand magnet from the studied samples. It is characterized by an opaque and black color rounded to sub-rounded grains and strongly magnetic (Figure 5a). These mineral constituents range from 1.6% to 10.9% with an average 6.1%, and represented by histogram figure 5b.

Ilmenite ([$FeTiO_3$])

It is commonly angular to subrounded grains with metallic luster, black to brownish black colors (Figure 5c). Ilmenite is the most abundant Fe-Ti oxide mineral that occurs in a wide variety of igneous rocks. This mineral constituents ranging from 1.7% to 11.9% with an average 6.7%, and represented by histogram figure 5d .

Rutile (TiO_2)

Rutile grains are subhedral to anhedral prismatic, tabular and elongated grains, varying in color from foxy red to reddish brown to opaque (Figure 5e). Rutile was recorded mostly in the non-magnetic fractions at 1.5 amp. and the magnetic fraction at 1.5 amp. Rutile is the preferred mineral for the production of titanium dioxide. This mineral constituents ranges from 0.2% to 3.9% with an average 2%, and represented by histogram figure 5f.

Table 3: The percentages of the heavy minerals of Wadi Yoider.

Sample No	Heavy minerals %	Sample No	Heavy minerals %
1	38	11	32.8
2	47.8	12	30.1
3	44.3	13	26.2
4	48.5	14	25.2
5	44.1	15	23.7
6	46.8	16	20.4
7	46.5	17	19.1
8	47.1	18	18.6
9	43.9	19	14.4
10	40.9	20	12.8
Min.	12.8		
Max.	48.5		
Aver.	30.86		

Leucoxene

Indeed leucoxene is an alteration product of ilmenite and is the transition stage between ilmenite and the secondary rutile. It is composed mainly from minute crystals of brookite and anatase. The leucoxene commonly occurs as rounded grains, opaque in transmitted light.

A rough pitted surface is the characteristic phenomena of most grains. The color of leu-

Table 4 The distribution of heavy minerals percentage in the study samples

S. No.	Mgt. %	Ilm.%	Rut. %	Leuc.%.	Gar. %	Tita. %	Zr. %	Mz%	Green Silicate %	Total Heavy
1	7.8	8.8	2.2	1.5	0.41	1.7	0.41	0.06	15.1	38
2	8.8	11.8	2.9	1.8	0.5	3.7	0.3	0.09	17.9	47.8
3	9.5	9.9	2	1.9	0.7	3.6	0.9	0.09	15.7	44.3
4	10.9	10.9	3.1	1.6	0.9	3.7	1.2	0.06	16.1	48.5
5	10.4	11.9	3.3	2.4	0.6	2.9	0.8	0.09	13.3	45.7
6	9.6	11	3.7	2.7	0.9	3	1.5	0.08	14.4	46.8
7	9.4	10.7	3.4	3	0.8	3.5	1.7	0.07	14	46.6
8	10.7	11.8	4	2.1	0.7	2.7	0.8	0.06	14.2	47.1
9	8.6	10.7	3.9	2.2	0.5	2.5	1	0.07	14.5	43.9
10	6.7	10.7	3	2.3	0.7	2.2	0.9	0.08	14.4	40.9
11	5.8	8.5	1.7	1.1	0.2	0.9	0.1	0.04	14.4	32.7
12	4.9	7.7	1	1.3	0.3	0.7	0.05	0.03	14.1	30.1
13	3.6	6.5	1.1	1.1	0.2	0.6	0.04	0.03	13	26.2
14	2.7	5.8	0.9	1.4	0.2	0.5	0.98	0.04	12.7	25.2
15	3.7	5.5	0.7	1.5	0.1	0.3	0.125	0.05	11.7	23.7
16	2.5	4.9	0.5	1	0.3	0.05	0.1	0.04	11	20.4
17	1.9	3.9	0.7	1.6	0.3	0.08	0.05	0.02	10.5	19.1
18	1.8	2.9	1.4	1.2	0.3	0.09	0.09	0.05	10.7	18.5
19	1.6	1.9	0.4	0.9	0.2	0.02	0.07	0.03	9.1	14.2
20	1.7	1.7	0.2	0.8	0.1	0.01	0.01	0.02	8.1	12.6
Min.	1.6	1.7	0.2	0.8	0.1	0.01	0.01	0.02	8.1	12.5
Max.	10.9	11.9	3.9	2.7	0.9	3.7	1.7	0.09	17.9	53.7
Aver.	6.1	6.7	2	1.7	0.48	0.76	0.05	1.7	12.5	88.1

coxene grains from the Egyptian black sands varies from white, yellowish white to brown, it depends mainly on the degree of alteration, (Figure 6a). Ibrahim (1995) stated that, if the iron content decreases, the grain color becomes lighter brownish yellow, yellow, yellowish white and light creamy colors. Its specific gravity ranging from 3.5 to 4 according to the number of vugs formed in grains through iron withdrawal processes. These mineral content range from 0.8% to 2.7% with an average 1.7%, and represented by histogram figure 6b.

Garnet

Garnet crystallizes in the isometric system, is mainly formed of angular to subrounded particles. Its grain size is relatively coarser than the other economic minerals of the study samples. Garnet is pale pink color (Figure 6c), and has moderate magnetic susceptibility. These mineral constituents range from 0.1% to 0.9 % with an average 0.48% and represented by histogram figure 6d.

Titanite [$CaTiSiO_5$]

Sphene is widespread in acidic and intermediate igneous rocks, and in several metamorphic rocks as accessory minerals. Titanite mineral grains are subhedral to anhedral grains of adamantine luster and imperfect cleavage. It exhibits transparent to translucent yellow to yellowish brown colors (Figure 6e). These minerals constituents ranges from 0.01% to 3.7% with an average 1.7%, and represented by histogram figure 6f.

Zircon [$ZrSiO_4$]

It occurs as subhedral to anhedral grains exhibiting colorless to brownish yellow colors of adamantine luster. Prismatic crystals are the prominent forms of zircon (Figure 7.a), while few zircon grains are well preserved as euhedral crystals with bipyramidal termination. These

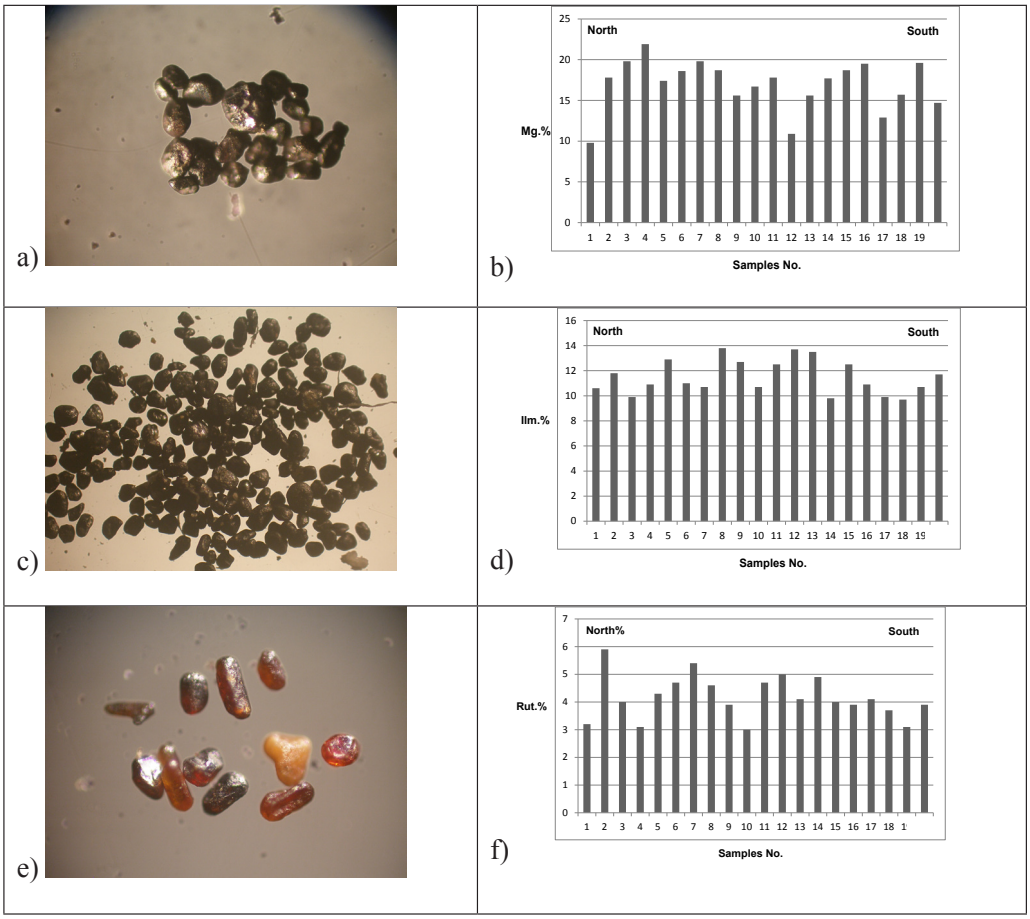

Figure 5 Show a)Photomicrographs of Magnetite b)Histogram of Magnetite % c) Photomicrographs of Ilmenite d) Histogram of Ilmenite% e) Photomicrographs of Rutile f) Histogram of Rutile%

minerals constituents range from 0.01 % to 1.7 % with an average 0.76 %, and represented by histogram figure 7b. The Semi quantitative analyses (EDX) of zircon is show in figure 7c.

Autunite $\{Ca(UO_2)_2(PO_4)_2nH_2O$ Hydrated Phosphate of calcium and hexavalent uranium

Autunite is one of the most abundant and widespread of the secondary mineral, and has constituted an important source of uranium at some localities. It is formed at essentially ordinary conditions of temperature and weathering of hydrothermal veins or other deposits carrying primary uraninite.

Thin to thick tabular with a rectangular or less commonly, an octagonal outline. The lateral faces usually are striated or serrated. The color is usually lemon yellow to sulfer yellow; sometimes greenish yellow to pale yellow (Figure 7d). It is characterized by transparent to translucent, specific gravity 3.05-3.2, and Hardness 2-2.5, luster vitreous, and pearly. Strong fluorescence to yellowish green in ultraviolet light (Iimori and Iwase, 1938; Meixner, 1940). Weathered surfaces sometimes are not fluorescent or only weakly fluorescent, a bright fluorescence appears on the fracture surfaces.

In natural material, nH_2O ranges zeolitically between about $10H_2O$ and $12H_2O$ but the upper limit may be higher. Autunite is fusible, and easily soluble in acids. It is very slightly soluble in water (Starik et al 1941).

Monazite [$CePO_4$]: is one of the most important nuclear minerals, being a major host for REEs and actinides Th and U (Hinton and Paterson 1994, Bea et al. 1994, Bea 1996). Monazite in the studied samples is rare constituting 0.074% of the heavy minerals of these samples. It forms rounded to well-rounded pale yellow, honey yellow, greenish yellow and reddish yellow grains (Figure. 7e). The absorption spectrum of monazite is determined mainly by Nd and Pr elements, Fe^{3+}, Fe^{2+} oxides content are the rea-

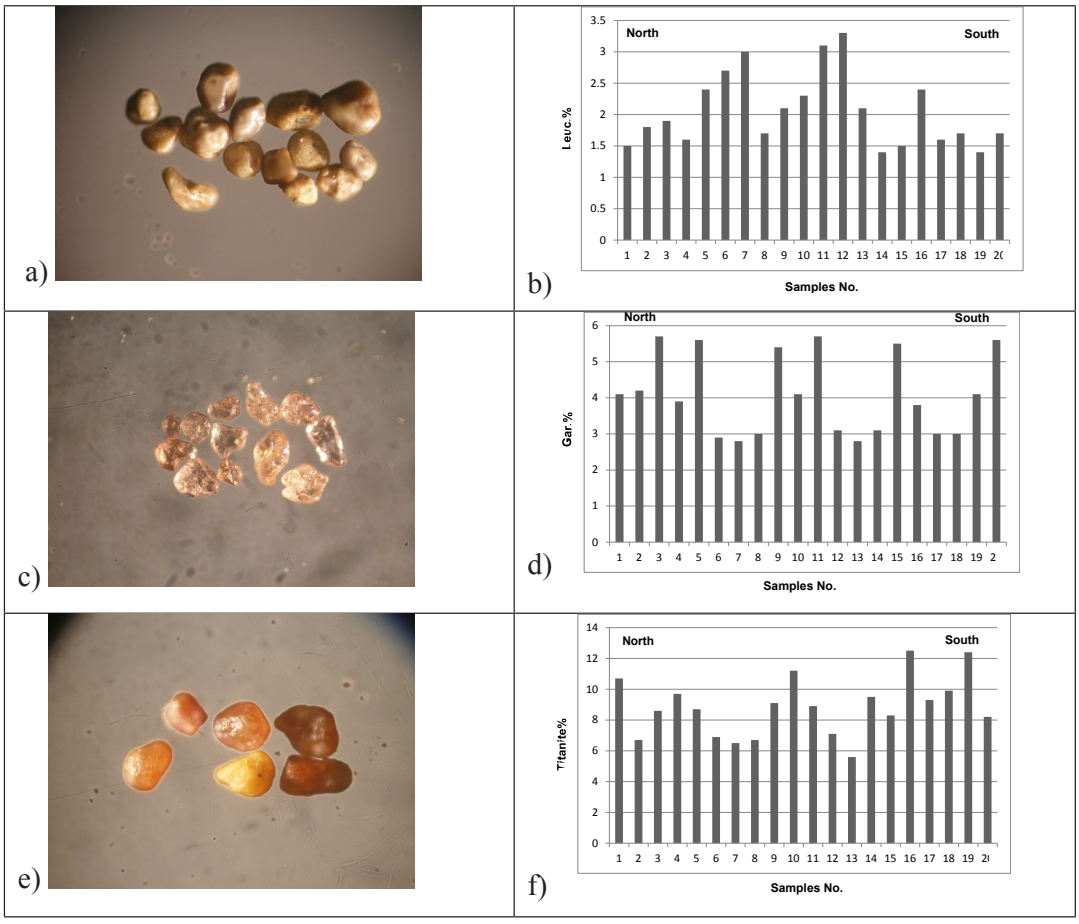

Figure 6 Show a) Photomicrographs of leucoxene b) Histogram of leucoxene% c) Photomicrographs of garnet d) Histogram of garnet%) e) Photomicrographs of titanite f) Histogram of titanite%

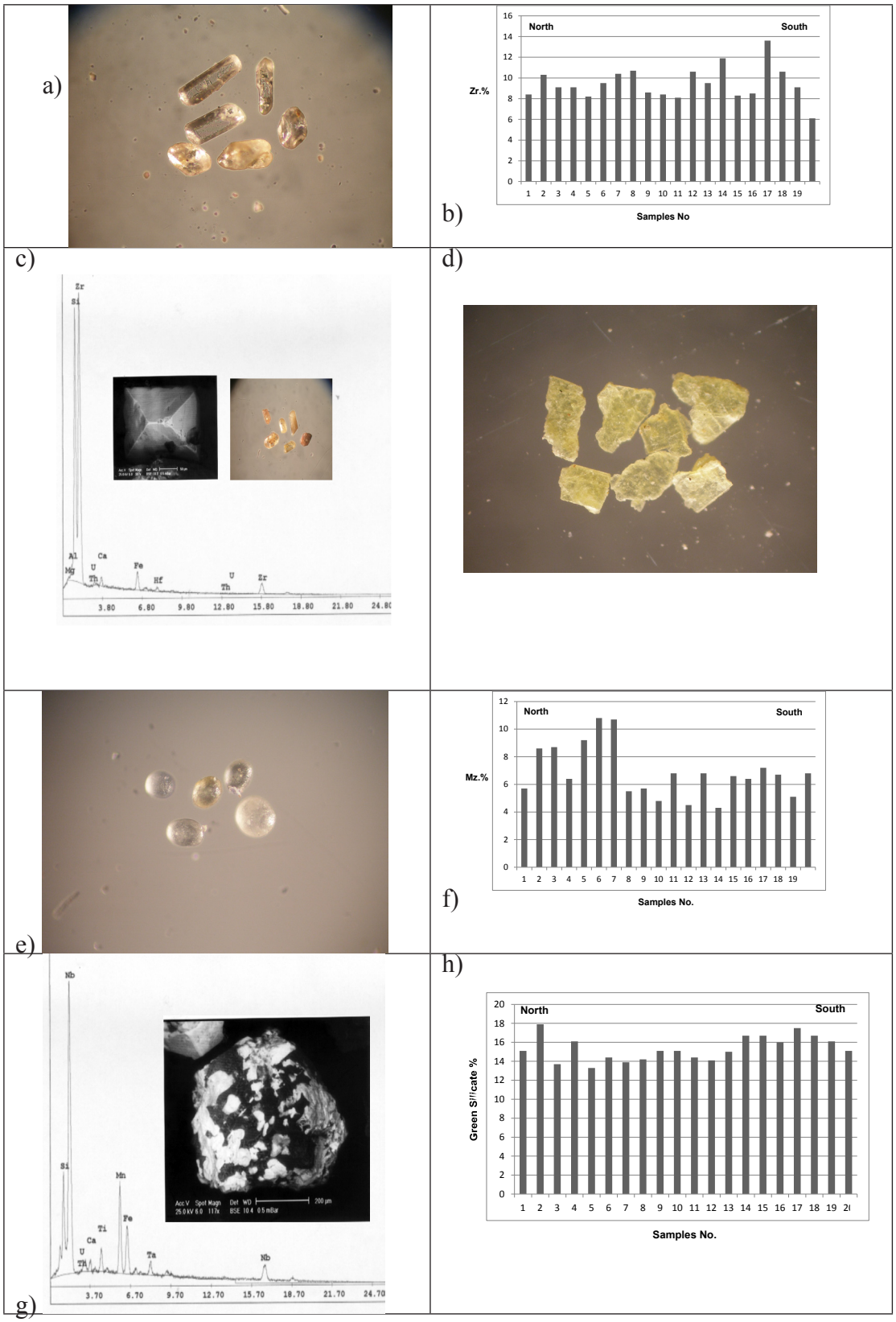

Figure 7 Show a) Photomicrographs of zircon b) Histogram of zircon % c) EDX and BSE of composite grain of zircon d) Photomicrographs of autunite e) Photomicrographs of monazite f) Histogram of monazite% g) EDX and BSE of composite grain of samarskite h)Histogram of green silicate.

son of coloration (Karavtchenko 1960). Most of these grains are characterized by pitted surfaces. They are range from 0.02% to 0.09%, with an average of 0.05%, and represented by histogram figure 7f**.**

Samarskite (Oxides and Hydroxides) **{(Y,Ce,U,Ca,Pb) $(Nb,Ta,Sn)_2O_6$}**

It is present as accessory mineral of many granitic pegmatite rich in rare earth elements and niobium. The crystals are rectangular prisms, striated, velvety-black with brown surface alteration. Also it is present as fracture filling in deformed zircon crystal. It is detected using EDX technique (Figure 7g).

Green Silicates

The common minerals in these groups are represented by biotites, hornblendes, muscovites, epidotes, augite, hypersthene, aegirine, diopside and enstatite. Other varieties are less common such as tremolite and actinolite. These minerals appears as yellowish green, dark green and green rod-like grains. These minerals have a wide range of magnetic susceptibility and most of them are moderately magnetic but hypersthene, aegerine and diopside are weakly magnetic while enstatite is non-magnetic. They are recorded in all samples of the studied stream sediments. They are range from 8.1% to 17.9%, with an average 12.5 %, and represented by histogram figure 7h.

Mineralogic Maturity

It is important as texture as a key of maturity of a sediment. Maturity as related to the mineral-components is known as "Mineralogic Maturity". Amineralogically mature sediment is that composed of a very few number of mineral species or even one species. It is the highly resistive mineral among the whole mineralogic assemblage that has been transported or deposited. On the other hand, a mineralogically immature sediment is that having stable and unstable minerals, monomineralic and polymineralic grains.

As the sediment is transported, the unstable minerals are abraded or dissolve to leave more stable minerals, such as quartz. Mature sediments, which contain stable minerals, generally have a smaller variety of minerals than immature sediments, which can contain both stable and unstable minerals. One measure of this maturity is the ZTR index which is a measure of the common resistant minerals found in ultra-weathered sediments: zircon, tourmaline, and rutile. The ZTR index is the percentage of the combined zircon, tourmaline, and rutile grains among the transparent, non-micaceous, detrital heavy minerals. Because of their high mechanical and chemical stability, zircon, tourmaline, and rutile are concentrated with quartz plus and chert.

A sedimentary sample from the lower (downstream) portions of a stream is likely to be more mature than one found upstream, since the original sediment has been subjected to more abrasion as it travels downstream.

Stream Sediments Geochemistry

The results of XRF analysis of trace elements for the investigated stream sedimentry samples are tabulated in table (5). The table shows that, the stream sedimentary samples are rich in Zr, Nb, Zn, Cu, Y, U and Th. These elements represent more higher than the representative elements average in earth crust. The other elements represent the lower concentration than the average in the earth crust. This clear that, the stream sediments are highly affected by the contribution of surrounding rocks. The distribution and lateral distribution of Zr, Nb, Y, U, and Th elements are shown Figures 8a, 8b, 9a, 9b, 10a, 10b, 11a,

Radiometric Study

A total of 20 stream sedimentary samples had been collected from the studied area throughout systematic sampling to determine variations in eU, eTh, Ra and K. The obtained results from the radiometric measurements of the studied stream sediments are listed in Table 5, and calculate the minimum, maximum, and average tabulated in table 6.

The examined stream sediments of Wadi Yoider are characterized by radiometrically mea-

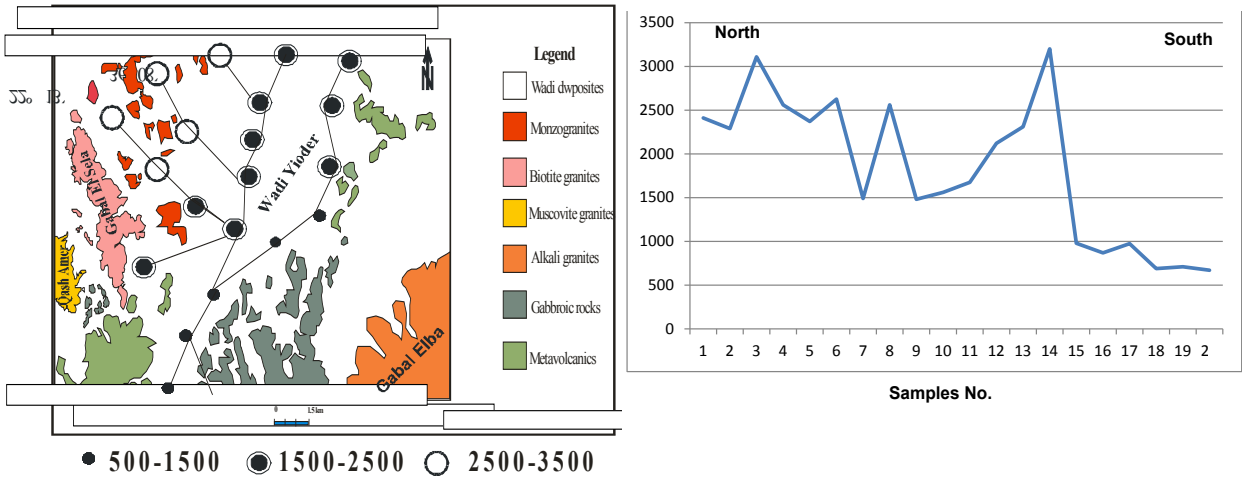

Figure 8 The distribution map of zircon in Wadi Yoider area b) Lateral distribution of zircon

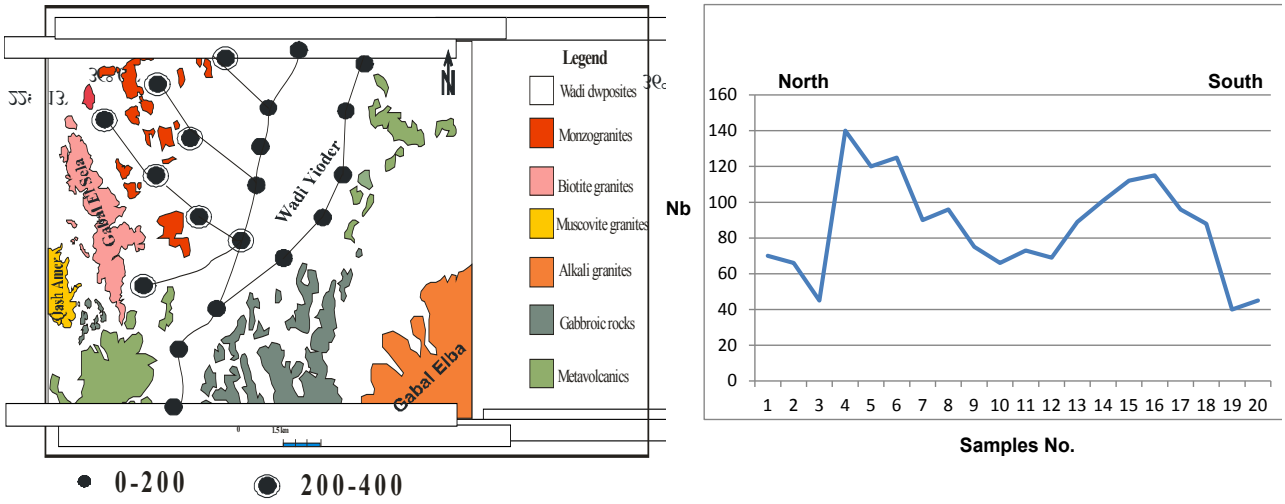

Figure 9 The distribution map of Nb in Wadi Yoider area b) Lateral distribution of Nb

Table 5 Concentrations of the analyzed trace elements (ppm) in the stream sedimentary samples in Wadi Yoider area, SED, Egypt. (Average earth crust = AVECS).

S. No.	Rb	Zr	Nb	Zn	V	Cu	Sr	Ba	Y	Ni	Ga	Cr	Pb	U	Th	K%	Th/U	Ra (ppm)	ARs eU/ Ra)
AVECS	90	163	20	70	120	60	370	425	33	84	19	102	14	4	12	20.9	----	----	-----
1	75	2110	175	311	112	71	50	60	110	20	10	12	8	8	19	2.4	2.4	4	2
2	85	2400	186	315	120	94	60	85	185	28	15	19	9	29	45	3.6	1.6	5	5.8
3	99	3620	250	364	122	115	65	81	186	25	25	17	11	26	60	4.6	2.3	4	6.5
4	95	2670	275	428	142	122	70	87	179	30	21	16	12	22	53	3.8	2.4	6	3.7
5	84	3350	250	335	105	112	79	93	178	27	23	15	13	25	51	2.9	2.04	3	8.3
6	89	2625	175	325	102	120	88	72	141	22	30	15	15	24	56	3.7	2.3	7	2.4
7	95	2395	140	219	100	100	79	76	138	21	35	16	19	23	50	3.2	2.2	3	7.7
8	65	2500	140	125	89	74	44	61	94	16	17	15	11	9	21	2.5	2.3	8	1.2
9	62	1750	95	112	82	82	53	64	78	17	18	12	9	10	23	2.3	2.3	7	1.4
10	75	1250	98	187	77	78	49	60	75	14	19	10	10	19	32	3.8	1.7	9	2.1
11	80	2675	145	279	100	97	85	75	112	30	22	19	18	25	42	4.7	1.7	10	2.5
12	75	2250	130	155	121	95	74	76	115	29	21	17	17	18	28	3.1	1.6	7	2.6
13	62	1315	105	91	95	80	65	58	94	17	15	13	11	10	15	2.2	1.5	15	0.7
14	73	1120	88	101	91	76	61	52	77	16	16	14	10	8	14	2.7	1.8	6	1.3
15	92	1700	256	345	147	118	78	75	70	28	22	20	18	35	65	5.3	1.9	4	8.8
16	99	1860	375	387	165	121	81	86	175	34	29	22	16	40	78	5.1	1.95	3	13.3
17	77	995	392	294	95	78	58	62	185	22	17	14	12	22	49	2.9	2.2	18	1.2
18	85	885	85	128	89	72	55	55	112	20	15	16	15	25	60	2.6	2.4	19	1.3
19	90	850	86	112	78	84	69	54	77	18	16	18	17	15	45	3.5	3	6	2.5
20	85	895	87	109	81	75	60	58	54	19	18	16	15	11	37	2.7	3.4	5	2.2

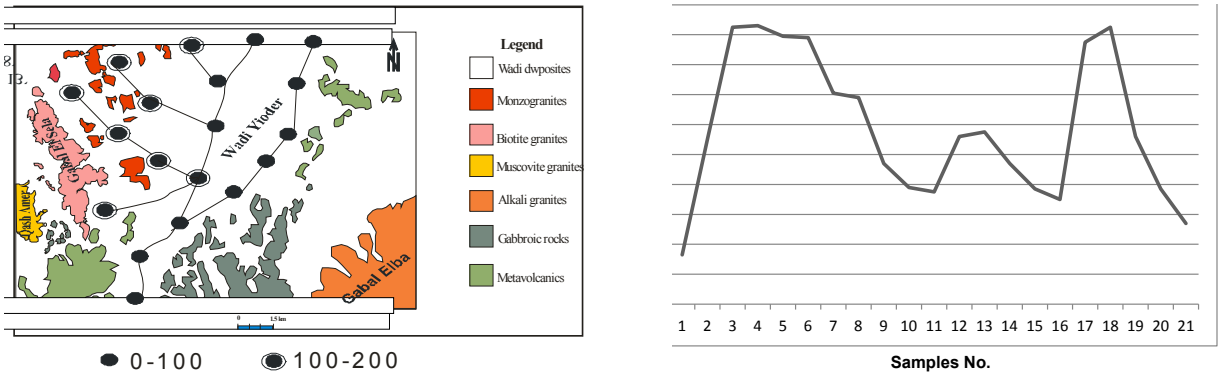

Figure 10 The distribution map of Yatrium in Wadi Yoider area b) Lateral distribution of Y

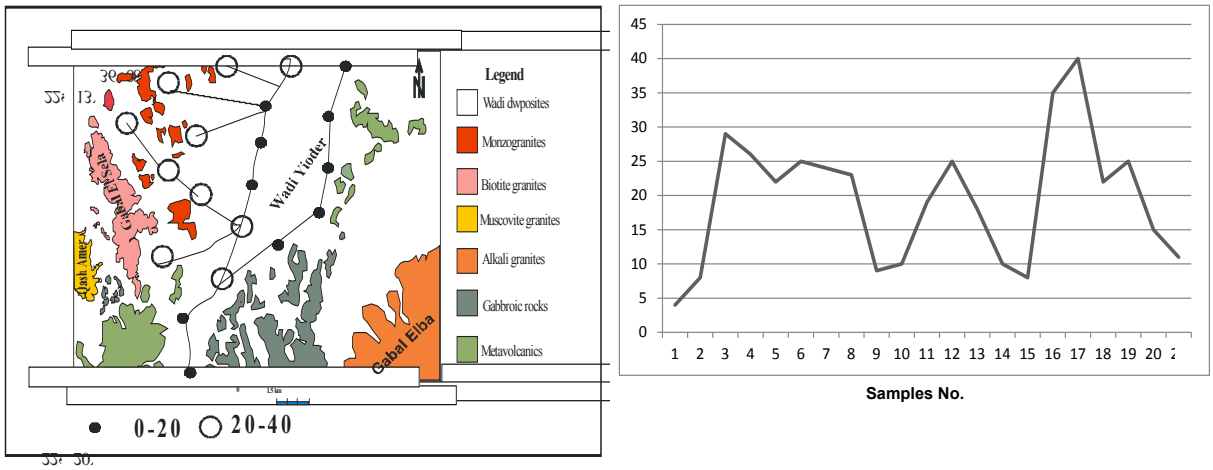

Figure 11 The distribution map of U in Wadi Yoider area b) Lateral distribution of U

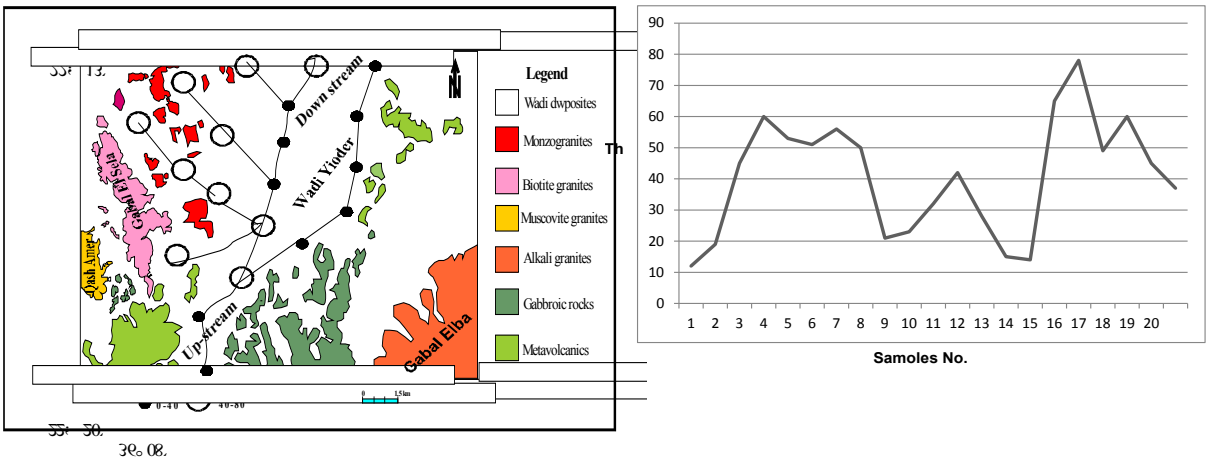

Figure 12The distribution map of Th in Wadi Yoider area b) Lateral distribution of Th

sured of elemental concentrations of eU ranging from 8 to 40 ppm with an average 20.2ppm (Figure 13a), while Th ranges from 14 to 78 ppm with an average 42.2ppm (Figure 13b), Ra ranging from 3 to 19 ppm with average 8.5ppm, and

Table 6 The distribution of radiomtric measurements of the studied stream sediments

Sample No.	eU (ppm)	eTh (ppm)	eTh/ eU	Ra (ppm)	ARs eU/ Ra)	K (%)
Min.	8	14	1.5	3	0.7	2.3
Max.	40	78	3.4	19	13.3	5.3
Aver.	20.2	42.2	2.2	8.5	3.9	3.3

K ranging from 2.3% to5.3 % with an average 3.3%.

Ivanovich (1994) concluded that a relatively constant eTh/eU mass ratio of around 3.5 is found in most natural systems, while the corresponding value obtained for this ratio is ranging from 1.5 to 3.4 with an average 2.2. Which indicate that there is a significant fractionation during weathering and transportation of these sediments.

The main factors controlling the distribution of radioelements in sediments are the geomorphological features of the basin of deposition, radioelements content of the source rocks, grain size of these sediments, the alkalinity of the surface groundwater, and to a lesser extent effect of the organic matter. $^{238}U/^{226}Ra$ activity ratios (ARs) can be used to ascertain equilibrium within the same decay series (Navas et al., 2002). If secular equilibrium prevails in the ^{238}U chain, Ars of $^{238}U/^{226}Ra$ will be approximately 1, Ars values other than 1 indicate disequilibrium. The Ars for the studied stream sediments of Wadi Yoider is higher than 1, which indicate a state of disequilibrium in these sediments.

eU versus eTh variation diagram

The relation between U and Th may indicate the enrichment or depletion of U because Th is chemically stable. The eU against eTh variation diagram for the studied samples is shown in Figure (13c), which indicates strong positive relationships between the two elements. This result explains the low alteration processes affecting on these samples, and also indicates that magmatic processes played an important role in the uranium enrichment of these granites which represent the source of these sediments.

eU vs eTh/U variation diagram

The bivariate diagram of eU against eTh/U is shown in Figure (13d). From this diagram, there are negative relationships for the studied samples. This relation may be attributed to the mobilization of uranium in the studied samples.

eTh versus eTh/eU variation diagram

The relation between eTh and eTh/eU ratios is shown in figure (13e) for the studied samples. This figure shows a scatter pattern which may be due to the effect of mobilization of (U) and concentration of (Th).

eU versus Zr variation diagram

The eU versus Zr variation diagram shows strong positive correlation in the studied samples (Figure 13f). The uranium and zirconium enrichment in the studied samples, supports the concept that U was trapped in the accessory minerals as zircon and the uranium is magmatically.

CONCLUSION

The area is covered by igneous rocks represented by different varies of granites cutted by different types of dikes and vein. Grain size analyses revealed that: The grain size ranges from medium to coarse sand and poorly sorted. These samples are characterized by fine skewed, near skewed, coarse skewed, platykurtic and mesokurtic. The stream sediments in the study area are affected by the source rock and turbulant transportation

The economic minerals are represented by magnetite, ilmenite, rutile, titanite, garnet, zircon, monazite, sphene, autunite, and samarskit. The distribution of some elements in the study area it is clear that they are concentrated near the outcrops of granites. The average radiometric measurements of stream sediments in the area represented by U, Th and concentrated 20.2 ppm and 42.2ppm respectively. These U and Th high contents may be due to the present of zircon, monazite, autunite, samarskit, and sphene.

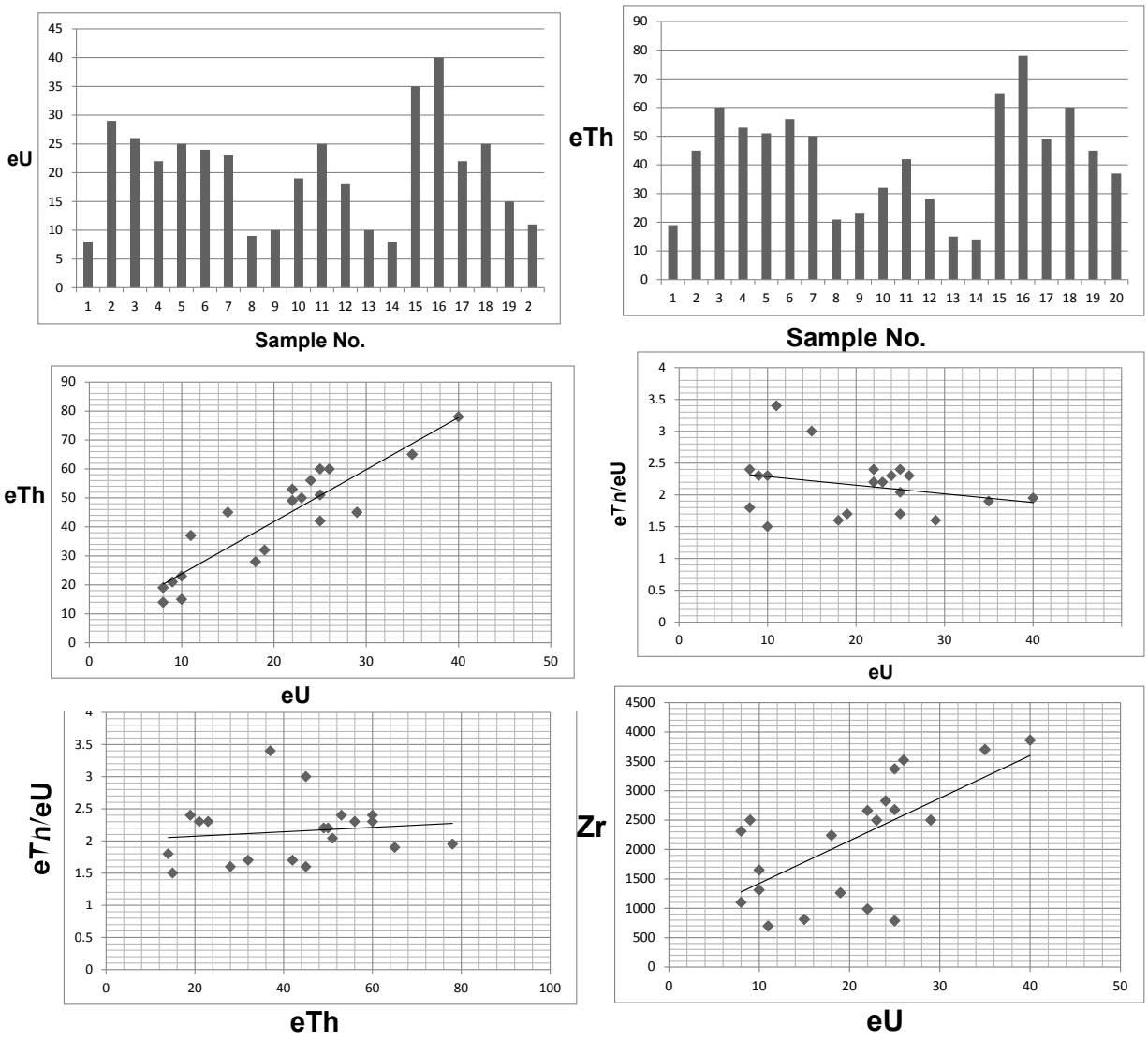

Figure 13: (a) and (b) Histograms showing the distribution of equivalent uranium and thorium ppm. (c) The relationship between equivalent uranium and equivalent thorium. (d) The relationship between eU and eTh/eU variation diagram for the stream sediments. (e) The relationship between eTh and eTh/eU variation diagram for the stream sediments. (f) The relationship between eU and concentration of Zr minerals.

REFRENCES

Abdel Meguid A. A., Cuney M., Ammar S. E., Ibrahim T. M. M., Ali Kh. G., Shahin H. A., Omer S. A., Gaafar I. M., Masoud S. M., Khamis A. A., Haridy M. H., Kamel A. I., Mostafa B. M., Abu Donia A. M. H., Abdel Gawad A. Aly E. M., 2003. Uranium Potential of Eastern Desert Granites, Egypt. Internal report, NMA, Cairo, Egypt.

Bea, F., 1996. Residence of REE, Y, Th and U in granites and crustal protolith; implications for the chemistry of crustal melt. J. Petrol., Vol. 37, P. 521:552.

Bea, F., Pereira, M. D., Corretage, L. G. and Fershtater, G. B., 1994. Differentiation of strongly peraluminous, perphosphorous granites: the Pedrobenards pluton, Central Spain. Geochemica et Cosmochemica Acta, Vol. 58, P. 2609:2627.

El-Gaby, S., List, F. K. and Tehrani, R., 1988. Geology, evolution and metallogenesis of the Pan-African Belt in Egypt, In: El-Gaby, S. and Greiling, R. O. (eds), The Pan-African Belt of Northeast of Africa and adjacent area. Tectonic evolution and economic aspects of Late Proterozoic Orogeny. Frieder Vieweg and Sohn, Braunschweig/Wiesbaden, pp. 18 - 68.

Folk, R. L., and Ward, W. C., 1957. Brazos River bar: a study in the significance of grain size parameter. Jour. Sedim. Petrol., V. 27, pp. 3-27.

Gaafar, I. M., Michel Cuney, Ahmed Abdel Gawad, 2014. Mineral Chemistry of Two-Mica Granite Rare Metals: Impact of Geophysics on the Distribution of Uranium Mineralization at El Sela Shear Zone, Egypt. Open Journal of Geology

Hinton, R. W. and Paterson, B. A., 1994. Crystallization history of granitic magma: evidences from trace elements zoning. Mineral. Mag., Vol. 58A, P. 416:417.

Ibrahim M. I. M., 1995. Investigation of some physical properties of zircon and rutile to prepare high purity mineral concentrates from the black sand deposits. M.Sc. Thesis, El Mansoura Univ. Egypt.

Iimori, S., and Iwase, E., 1938. The fluorescence spectrum of autunite: Tokyo Inst. Phys. Chem. Research Sci Paoer, v. 34, p. 372.

Ivanovich, M., 1994. Uranium series disequilibrium: concept and applications. Radiochem. Acta, Vol. 64, P. 81:94.

Karavtchenko, G. T., 1960. Colouration of monazite. Akad. Nauk. USSR, Sibir., Octdec. No. 7, P. 80:90.

Kroner, A., 1984. Late Precambrian plate tectonics and orogeny, a need to redefine the term Pan-African. In: Klerkx, J. and Michot, J. (eds.), African Geology, Tervuren, pp. 23-28.

Matolin, M., 1990. A report to the Government of the Arab Republic of Egypt "Construction and use of spectrometric calibration pads", Egypt/4/030-03, Laboratory Gamma Ray spectrometry

Meixner, H., 1940. Notizen uber neue Vorkommen einiger Uranminerale: Zentralbi. Mineralogie-1940, Abt. A, p. 145-148.

Navas, A., Soto, J. and Machin, J., 2002. ^{238}U, ^{226}Ra, ^{210}Pb, ^{232}Th and ^{40}K activities in soil profiles of the Flysch sector (Central Spanish Pyrenees). Applied Radiation and Isotopes. Vol. 57, P. 579:589.

Starik, I. E., Samartzeva, A. G., and Yashch enko, M. R. S. S., 1941. Solubility of secondary uranium minerals: Acad. Sci. U. R. S. S.., Comptes rendus, V. 31, P. 909-910.

Stern, R. J., Gottfried, D. G. and Hedge, C. E., 1984. Late Precambrian rifting and crustal evolution in the north eastern Desert of Egypt. Geology 12, pp 168 - 172.

دراسات معدنية واشعاعية لرواسب منطقة وادى يودر-جنوب الصحراء الشرقية-مصر

مصطفى بيومي – اشرف العزب- خالد الحسيني

تقع منطقة وادى يودر بالقرب من جبل سيلا جنوب الصحراء الشرقية وتشمل هذه المنطقة على

البركانيات القديمة المتحولة والجابرو الحديث ثم صخور الجرانيتات الحديثة المقطوعة بالجدد الحامضية ومغطى بالرواسب الحديثة التى تملاء وديان المنطقة. ويعتبر وادى يودر الوادى الرئيسى بالمنطقة ويتفرع منه عدة اودية اصغر. وقد تم دراسة الحجم الحبيبي لرواسب هذه الوديان حيث وجد ان هذه الرواسب تنحصر بين الحجم المتوسط والكبير ومعامل التفلطح المتوسط والمستعرض كما وجد ان محتوى وصفات هذه الرواسب يتأثر بمصدر الصخور وعامل النقل المتمثل بالتيارات العكرة.

ومن دراسة المحتوى المعدني لهذه الرواسب يتمثل بوجود بعض المعادن الاقتصادية مثل الماجنتيت والالمينيت والروتيل والجارنت والتيتانيت ومعادن حاملة للعناصر المشعة مثل الزيركون والمونازيت والاوتونيت والسمارسكيت. وتتركز هذه المعادن في وسط وشمال الوادي (المصب) بالقرب من صخور الجرانيت بجبل سيلا. وهى معادن مقاومة لعوامل التعرية.